

Branched polymers in the presence of impurities

Markus Porto,¹ Arkady Shehter,² Armin Bunde,^{1,2} and Shlomo Havlin^{1,2}

¹*Institut für Theoretische Physik III, Universität Giessen, Heinrich-Buff-Ring 16, D-35392 Giessen, Germany*

²*Minerva Center and Department of Physics, Bar-Ilan University, 52900 Ramat Gan, Israel*

(Received 23 January 1996)

We study branched polymers in the presence of impurities using the *branched polymer growth model*, which has been proposed by Lucena *et al.* [Phys. Rev. Lett. **72**, 230 (1994)]. To avoid boundary effects we study the growth process in chemical *l*-space and determine the structural exponents d_l , d_{\min} , and τ . For $d=2$ (square lattice) and $d=3$ (simple cubic lattice) our results are based on numerical simulations, while for the Bethe lattice ($d=\infty$) the quantities of interest were obtained analytically. These results support our recent suggestion that on the critical line the branched polymers belong to the universality class of percolation. [S1063-651X(96)08607-2]

PACS number(s): 61.41.+e

I. INTRODUCTION

In recent years the problem of how polymerization occurs has been the subject of extensive experimental and theoretical studies [1–8]. There exists a large variety of polymer structures that generally depend on the external conditions and the type of interaction between the monomers. In this paper we focus on linear and branched polymers in dilute solutions, where interactions between the different polymers can be neglected. It is well known that linear polymers in dilute solution can be modeled by self-avoiding walk (SAW) chains, where the SAW ensemble consists of all configurations of nonintersecting random walks [1,2]. In recent years it was found that large SAWs can be generated by kinetic growth walks (KGWs), where at each step a random walker can move to a neighbor site that has not been visited before [9–11].

More recently, Lucena *et al.* [12] generalized the KGW to include branching [the branched polymer growth model (BPGM)]. In this model a branched polymer is generated from a seed in a d -dimensional lattice similar to the KGW, but at each step branching can occur with bifurcation probability b . In addition, not all lattice sites are available for the growing branched polymer, but a fraction q of them is blocked. Since the KGW model of linear polymers belongs to the universality class of linear polymers in dilute solutions [9–11], it is expected that its generalization, the BPGM, belongs to the universality class of branched polymers in dilute

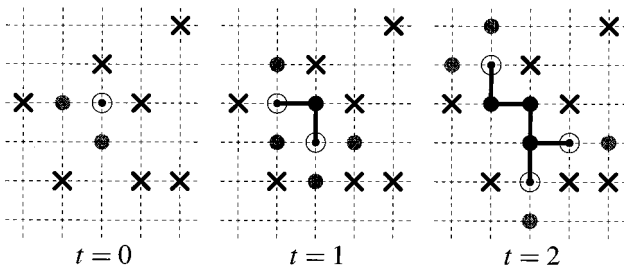


FIG. 1. Illustration of the first steps of a BPGM. Sites not available for the branched polymer are marked by a cross, polymer sites by a full circle, the active sites of the polymer by an open circle, and the growth sites by a gray circle.

solutions. It has been found by numerical simulations in a square lattice [12,13] that there exists a critical line $q_c(b)$ that separates a region where SAWs are grown from a region where compact structures are generated. It was suggested [13] that at the critical line the structures belong to the universality class of percolation. In this paper we extend our previous numerical study [13] to include three-dimensional systems and the Bethe lattice (Cayley tree). On the Cayley tree we calculate the critical line $q_c(b)$ rigorously. We also determine analytically the properties of the branched polymers at the critical line and show that their characteristic exponents are the same as for percolation.

The paper is organized as follows. In Sec. II we describe the BPGM and the quantities studied in this paper. Section III presents the numerical results for the square and the cubic lattice. In Sec. IV we present the analytical results for the BPGM on the Cayley tree. Section V, finally, concludes the paper with a discussion and a comparison of the BPGM to related models.

II. BRANCHED POLYMER GROWTH MODEL

Consider a d -dimensional lattice where each site has z nearest-neighbor sites. At $t=0$, the center of the lattice is

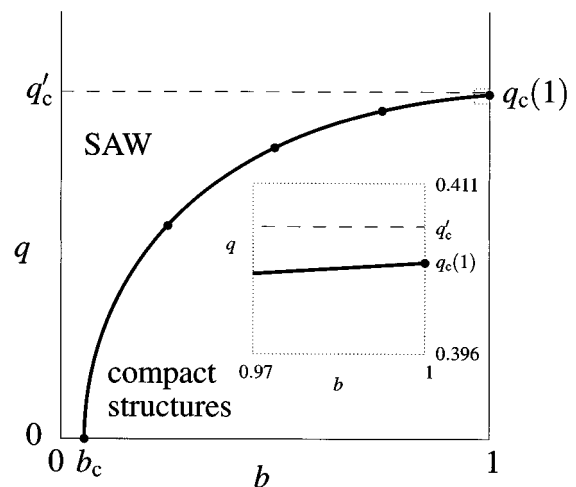


FIG. 2. Phase diagram for the BPGM in $d=2$. The inset is a magnification of the regime around the point $(b, q) = (1, q_c(1))$.

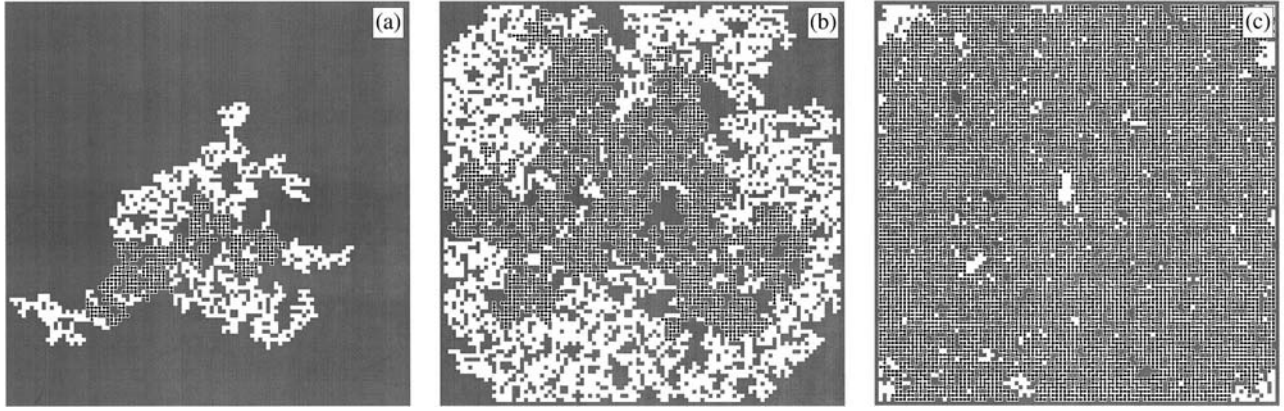


FIG. 3. Three typical branched polymers generated by the BPGM; (a) in the SAW regime; (b), $(b, q) = (0.5, 0.4072)$; (b) on the critical line, $(b, q) = (0.5, 0.3415)$; and (c) in the compact regime, $(b, q) = (0.5, 0.2)$.

occupied by a monomer seed. There are z nearest-neighbor sites of the seed where other monomers can be added and the polymer can grow. At step $t=1$, two of these growth sites are chosen randomly. One of them is occupied by a monomer (with probability 1), the other one is occupied by a monomer with bifurcation probability b . In general, at step $t+1$ the polymer can grow from each of the monomers added at the foregoing step t to empty nearest-neighbor sites (growth sites), either in a linear fashion or by bifurcation with probability b . If there are no growth sites left, the polymer stops growing. If a certain concentration q of lattice sites is blocked by impurities, they cannot serve as growth sites. For $q=0$ and $b=0$, the model reduces to the KGW model. An illustration of the BPGM for the first steps is shown in Fig. 1.

For determining the structure of the branched polymers we studied the growth process in “chemical” l -space and determined the critical exponents d_{\min} and d_l [14], as well as the number of surviving polymers $N(t)$ as a function of the number of growth steps t . The chemical distance l between two monomers separated by an Euclidean distance r is defined as the minimum number of bonds connecting them on

the cluster. The fractal dimension d_{\min} describes how l scales with r , $l \sim r^{d_{\min}}$. The chemical dimension d_l describes how the cluster mass M scales with l , $M \sim l^{d_l}$, and is related to the fractal dimension d_f by $d_f = d_l d_{\min}$. For SAW structures we have $d_l = 1$, $d_{\min} = d_f \cong (d+2)/3$ ($d \leq 4$), and an exponential decay of the number of surviving polymers $N(t)$, while for compact structures ($d_f = d$), $d_{\min} = 1$, $d_l = d_f$, and $N(t) \rightarrow N(\infty) > 0$ for $t \rightarrow \infty$. For percolation clusters at the critical concentration, we have a power-law behavior $N(t) \sim t^{-\tilde{\tau}}$ or, since for the BPGM $t=l$, $N(l) \sim l^{-\tilde{\tau}}$ with $\tilde{\tau} = (\tau - 2)d_l = (d/d_f - 1)d_l$ [14], and $d_{\min} \cong 1.13$, $d_f = 91/48$, $d_l \cong 1.68$, and $\tilde{\tau} \cong 0.092$ for $d=2$, $d_{\min} \cong 1.37$, $d_f \cong 2.54$, $d_l \cong 1.85$, and $\tilde{\tau} \cong 0.35$ for $d=3$ and $d_{\min} = 2$, $d_f = 4$, $d_l = 2$, and $\tilde{\tau} = 1$ for $d \geq 6$. Above the critical dimension $d_c = 6$, percolation on a lattice can be modeled by percolation on the Cayley tree.

By definition, branched polymers are grown in chemical space: At step $t=1$, the first shell (with $l=1$) is grown, at step $t=2$, the second shell is grown, etc. (see Fig. 1). Hence the chemical space is the natural metric for calculating the critical exponents of the BPGM. In fact, by generating all

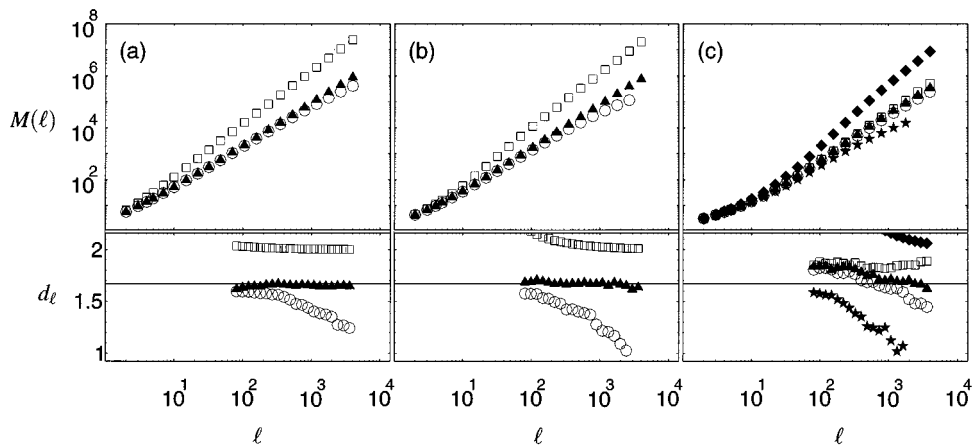


FIG. 4. Plot of the mass $M(l)$ and the corresponding chemical dimension d_l [obtained from successive slopes of $\log M(l)$ vs $\log l$] as a function of l for (a) $b=1$ and $q=0.2$ (square), 0.404 (full triangle), and 0.4072 (circle); (b) $b=0.5$ and $q=0.2$ (square), 0.3415 (full triangle), and 0.35 (circle); and (c) $q=0$ and $b=0.1$ (full diamond), 0.058 (square), 0.0565 (full triangle), 0.055 (circle), and 0.04 (full star). The horizontal lines represent the known value $d_l \cong 1.68$ for percolation in $d=2$. The simulations were performed on a square lattice and averages were taken over 5000 configurations.

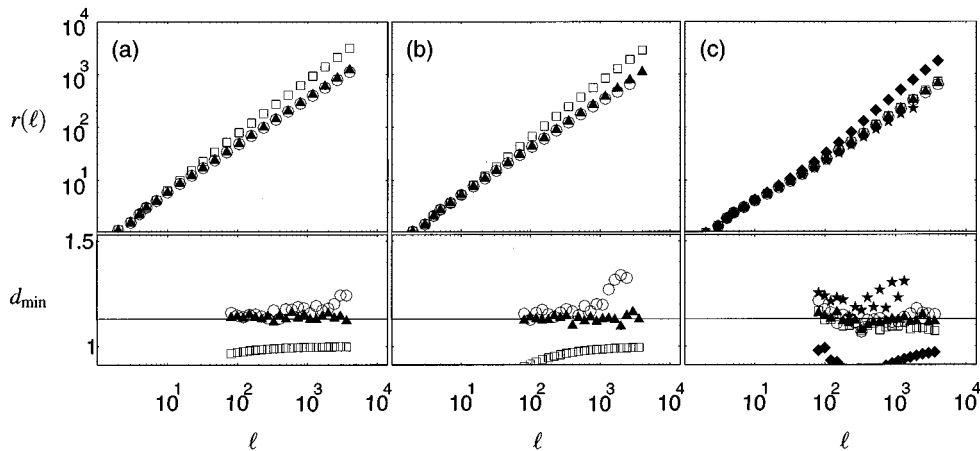


FIG. 5. Plot of the distance $r(l)$ and the corresponding fractal dimension of the shortest path d_{\min} [obtained from successive slopes of $\log r(l)$ vs $\log l$] as a function of l for the parameters described in Fig. 4. The horizontal lines represent the known value $d_{\min} \approx 1.13$ for percolation in $d=2$.

shells up to a certain chemical distance l we avoid the boundary effects present when measuring d_f directly from the mass-radius relation $M \sim r^{d_f}$.

III. NUMERICAL RESULTS IN TWO AND THREE DIMENSIONS

A. Square lattice ($d=2$)

Figure 2 shows the phase diagram and the critical line $q_c(b)$. The dashed line marks the percolation threshold $q'_c \approx 0.4072$ of the square lattice. Above this line only finite percolation clusters exist [14] and therefore only finite branched polymers can be generated. Below this line and above the critical line $q_c(b)$, the branched polymers belong to the universality class of SAWs, while below $q_c(b)$ compact structures with $d_f=d$ are grown. On the critical line the numerical results (see below) suggest that the branched polymers are in the universality class of percolation. Typical branched polymers in the three regimes are shown in Fig. 3.

Figure 4 shows the mean mass $M(l)$ of a branched polymer as a function of the chemical distance l in the vicinity of three representative points at the critical line: (a) around $b=1$ [$q_c(1) \approx 0.4037$], (b) around $b=0.5$ [$q_c(0.5) \approx 0.3415$], and (c) at $q=0$, around $b_c \approx 0.0567$ [$q_c(0.0567) \approx 0$].

Figures 5 and 6 show the mean Euclidean distance r of a monomer and the number of surviving polymers N as a function of its chemical distance l from the seed for the same

parameters as in Fig. 4. We observe three types of behavior for large l : Below the critical line we have $M(l) \sim l^2$, $r(l) \sim l$, and $N(l) \rightarrow N(\infty) > 0$ for $t \rightarrow \infty$, i.e., compact clusters with $d_f=2$ and $d_{\min}=1$ are generated. Above the critical line we have $d_f \rightarrow 1$ and $d_{\min} \rightarrow 4/3$, as well as an exponential decay of $N(l)$, representing the SAW universality class. At the critical line $q_c(b)$ the branched polymers have exponents very close to percolation, $d_f \approx 1.68$, $d_{\min} \approx 1.13$, and $\tilde{\tau} \approx 0.092$. The results are quite convincing for $b=1$ [Figs. 4(a), 5(a), and 6(a)] and for $b=0.5$ [Figs. 4(b), 5(b), and 6(b)], where the critical regime is reached already for small values of l . In the absence of impurities ($q=0$) and for b above criticality, however, there exist large crossover phenomena, since initially the number of monomers grows exponentially in the absence of impurities. This is clearly seen from Fig. 4(c) for $b=0.1$, where $d_f=2$ is approached from well above. From Figs. 4(c), 5(c), and 6(c) we find also that the critical point for $q=0$ is $b_c = 0.0570 \pm 0.005$ and the exponents, when extrapolated to $l \rightarrow \infty$, are $d_f = 1.70 \pm 0.05$, $d_{\min} = 1.10 \pm 0.05$, and $\tilde{\tau} = 0.09 \pm 0.01$, being consistent with the exponents of percolation.

Figures 4(a), 5(a), and 6(a) show that for $b=1$ (full bifurcation) the critical q value is $q_c(1) = 0.4040 \pm 0.0005$, which is well below the percolation threshold $q'_c \approx 0.4072$. The reason for the difference between q'_c and $q_c(1)$ is that higher-order branching (trifurcation, tetrafurcation) is forbidden, which effectively decreases $q_c(1)$. From this follows the surprising observation that even on the infinite percolation

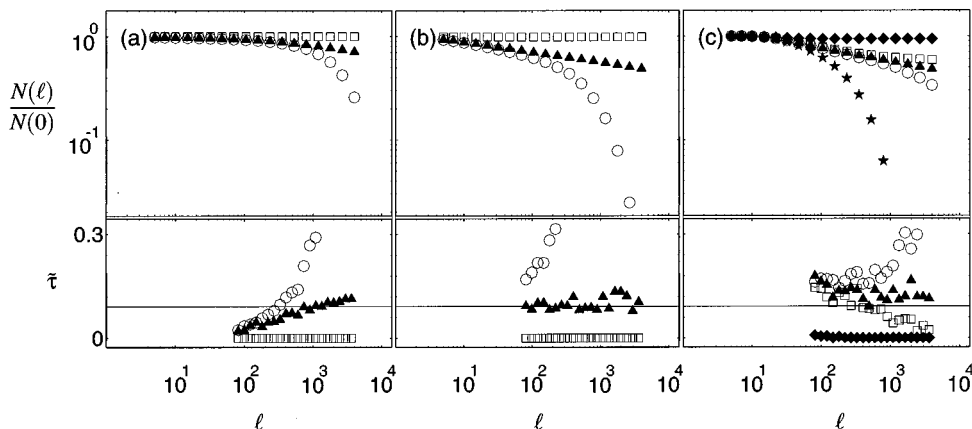


FIG. 6. Plot of the number of surviving polymers $N(l)$ and the corresponding exponent $\tilde{\tau}$ [obtained from successive slopes of $\log N(l)$ vs $\log l$] as a function of l for the parameters described in Fig. 4. The horizontal lines represent the known value $\tilde{\tau} \approx 0.092$ for percolation in $d=2$.

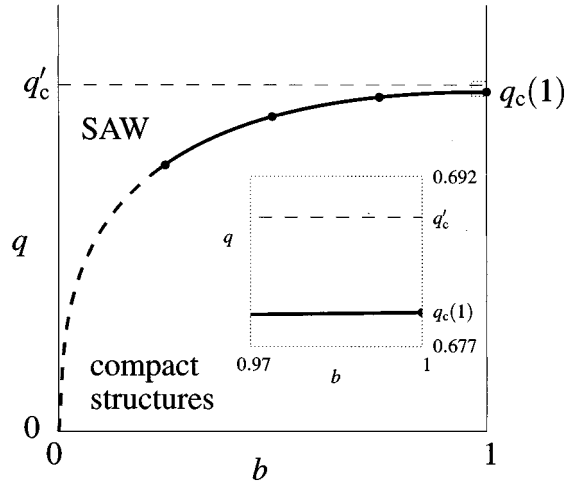


FIG. 7. Phase diagram for the BPGM in $d=3$. The inset is a magnification of the regime around the point $(b, q) = (1, q_c(1))$.

cluster below q'_c , which is compact on large length scales, branched polymers with bifurcation probability $b=1$ will also end up as SAW-type polymers, as long as $q > q_c(1)$. The difference between q'_c and $q_c(1)$ increases with increasing coordination number. An alternative model for branched polymers is to grow linear with probability 1 and to allow branching with probability b for *all* remaining available growth sites. In this case we expect that $q_c(1) = q_c$ for all dimensions.

B. Simple cubic lattice ($d=3$)

Figure 7 shows the phase diagram and the critical line $q_c(b)$ for the simple cubic lattice. The dashed line marks the percolation threshold $q'_c \cong 0.6884$ of the sc lattice. The dotted line is an extrapolation of that part of the critical line (full line) that has been obtained numerically. Due to numerical limitations, the properties of the branched polymer in the dotted line regime could not be determined with the sufficient accuracy.

Figure 8 shows the mean mass $M(l)$ of a branched polymer as a function of the chemical distance l , in the vicinity of three representative points at the critical line: (a) around $b=1$ [$q_c(1) \cong 0.680$], (b) around $b=0.5$ [$q_c(0.5) \cong 0.6275$], and (c) at $q=0$, around $b \cong 0$.

Figures 9 and 10 show the mean Euclidean distance r of a monomer and the number of surviving polymers N as a function of its chemical distance l from the seed, for the same parameters as in Fig. 8. As in Figs. 4–6 for $d=2$, we observe three types of behavior. Below the critical line we have $M(l) \sim l^3$, $r(l) \sim l$, and $N(l) \rightarrow N(\infty) > 0$ for $t \rightarrow \infty$, i.e., compact clusters with $d_l = 3$ and $d_{\min} = 1$ are generated. Above the critical line we have $d_l \rightarrow 1$ and $d_{\min} \rightarrow 5/3$, as well as an exponential decay of $N(l)$, representing the SAW universality class. At the critical line $q_c(b)$ the branched polymers have exponents very close to percolation, $d_l \cong 1.85$, $d_{\min} \cong 1.37$, and $\bar{\tau} \cong 0.35$. Again the results are convincing for $b=1$ [Figs. 8(a), 9(a), and 10(a)] and for $b=0.5$ [Figs. 8(b), 9(b), and 10(b)], where the critical regime is reached already for small values of l . In the absence of impurities ($q=0$) and for b close to 0, the results are not conclusive and from the numerical data it is not clear whether b_c is finite or 0. In the discussion (Sec. V) heuristic arguments are given that b_c is very small but finite. Figures 8(a), 9(a), and 10(a) show that for full bifurcation ($b=1$), $q_c(1) = 0.680 \pm 0.005$, which is below $q'_c \cong 0.6884$.

IV. BRANCHED POLYMERS ON THE CAYLEY TREE

Consider a Cayley tree with coordination number z , where each site is free with probability p and blocked with probability $q = 1 - p$. The mean number of sites on a cluster at chemical distance l from a center site is

$$g(l) = zp[(z-1)p]^{l-1}. \quad (1)$$

For $l \rightarrow \infty$, $g(l)$ decreases exponentially to 0 for $(z-1)p < 1$ and diverges for $(z-1)p > 1$. Therefore the condition

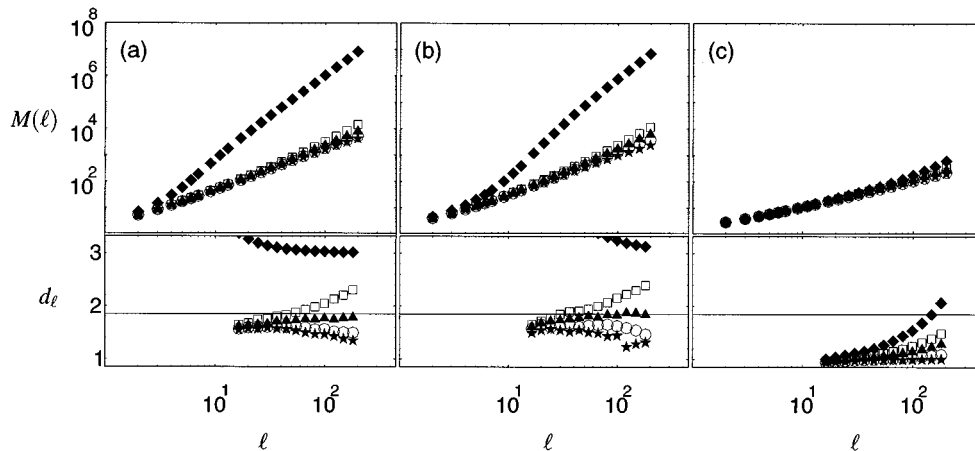


FIG. 8. Plot of the mass $M(l)$ and the corresponding chemical dimension d_l [obtained from successive slopes of $\log M(l)$ vs $\log l$] as a function of l for (a) $b=1$ and $q=0.2$ (full diamond), 0.675 (square), 0.68 (full triangle), 0.685 (circle), and 0.6884 (full star); (b) $b=0.5$ and $q=0.2$ (full diamond), 0.62 (square), 0.6275 (full triangle), 0.635 (circle), and 0.645 (full star); and (c) $q=0$ and $b=0.01$ (full diamond), 0.005 (square), 0.003 (full triangle), 0.001 (circle), and 0.0001 (full star). The horizontal lines represent the known value $d_l \cong 1.85$ for percolation in $d=3$. The simulations were performed on a simple cubic lattice and averages were taken over 5000 configurations.

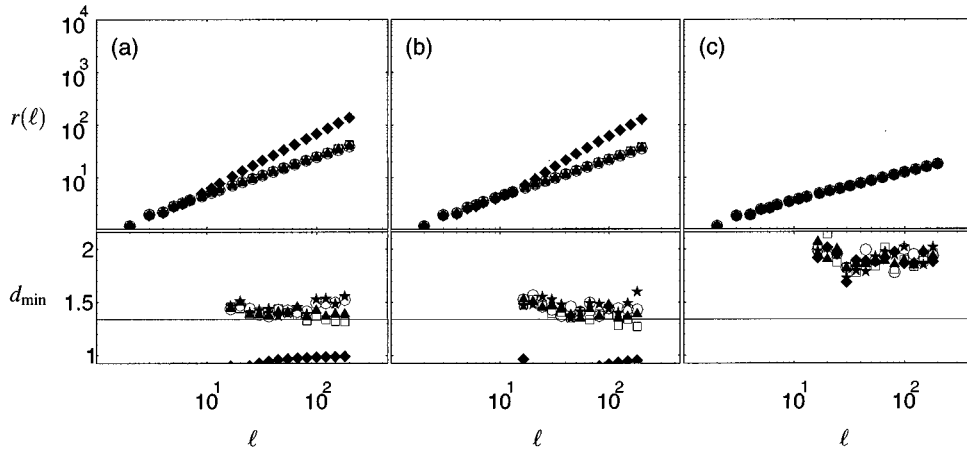


FIG. 9. Plot of the distance $r(l)$ and the corresponding fractal dimension of the shortest path d_{\min} [obtained from successive slopes of $\log r(l)$ vs $\log l$] as a function of l for the parameters described in Fig. 8. The horizontal lines represent the known value $d_{\min} \cong 1.37$ for percolation in $d=3$.

$$\lim_{l \rightarrow \infty} g(l) = \text{const} \neq 0, \infty \quad (2)$$

defines the critical point p_c , $(z-1)p_c=1$, or $p_c=(z-1)^{-1}$. The quantity in square brackets in (1), $G(z,p) \equiv (z-1)p$, specifies the mean number of cluster sites in shell $l+1$ that are connected to a cluster site in shell l . The probability that a cluster site in shell l has k neighbor sites in shell $l+1$ is

$$w_k = \binom{z-1}{k} p^k (1-p)^{z-1-k}. \quad (3)$$

Hence the mean number of sites generated by k branches from a site in shell l is kw_k and thus

$$\sum_{k=0}^{z-1} kw_k = (z-1)p. \quad (4)$$

In the BPGM, k can obtain the value 1 with probability $1-b$ and the value 2 with probability b . Hence, in the BPGM, the mean number of cluster sites in shell $l+1$ that are connected to a cluster site in shell l is

$$G_{\text{BPGM}} = (1-b) \left[\sum_{k=0}^{z-1} \min(k,1) w_k \right] + b \left[\sum_{k=0}^{z-1} \min(k,2) w_k \right]. \quad (5)$$

Using Eq. (3) it is easy to verify that the sums in (5) can be simplified to

$$G_{\text{BPGM}} = 1 + b[(z-2)q^{z-1} + (z-1)q^{z-2} + 1] - q^{z-1}. \quad (6)$$

The critical line $b_c(q)$ [which is the inverse function of $q_c(b)$] is obtained from the condition

$$G_{\text{BPGM}} = 1, \quad (7)$$

which yields

$$b_c(q) = \frac{q^{z-1}}{(z-2)q^{z-1} - (z-1)q^{z-2} + 1}. \quad (8)$$

Figure 11 shows $b_c(q)$ from Eq. (8). Note that $b_c(0)=0$ for all z , hence the point $(q=0, b=0)$ is on the critical line. If we approach this point from the q axis ($b=0, q \rightarrow 0$), we expect SAWs, if we approach it from the b axis ($q=0, b \rightarrow 0$), we expect compact clusters, and, as will be shown below, we expect percolation clusters if we approach it along the critical line.

For $b=1$, we have $q_c(1) = q'_c = \frac{1}{2}$ for $z=3$, while for $z>3$, $q_c(1)$ is smaller than $q'_c = 1 - 1/(z-1)$; see Fig. 11. As expected the difference $q'_c - q_c(1)$ increases with z . For the alternative model introduced in Sec. III we expect $q_c(1) = q'_c$ for all coordination numbers z .

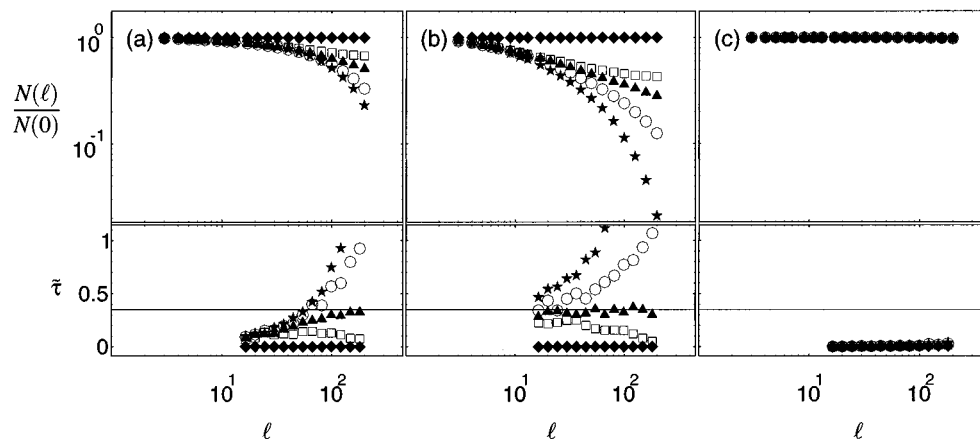


FIG. 10. Plot of the number of surviving polymers $N(l)$ and the corresponding exponent $\tilde{\tau}$ [obtained from successive slopes of $\log N(l)$ vs $\log l$] as a function of l for the parameters described in Fig. 8. The horizontal lines represent the known value $\tilde{\tau} \cong 0.35$ for percolation in $d=3$.

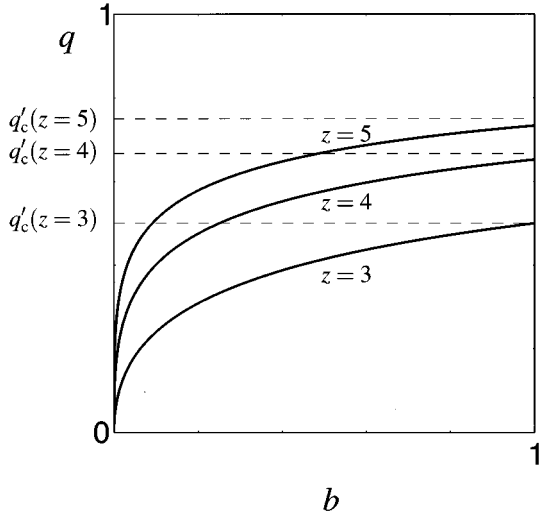


FIG. 11. Phase diagram for the BPGM on the Cayley tree, for coordination numbers $z=3,4,5$. The dashed lines represent the respective percolation thresholds $1/(z-1)$.

To see that the branched polymers on the critical line belong to the universality class of percolation, note that (6) can be written as

$$G_{\text{BPGM}} = (z-1)p^*, \quad (9)$$

with an effective percolation probability p^* ,

$$p^* = \frac{1}{z-1} + \frac{b[(z-2)q^{z-1} + (z-1)q^{z-2} + 1] - q^{z-1}}{z-1}. \quad (10)$$

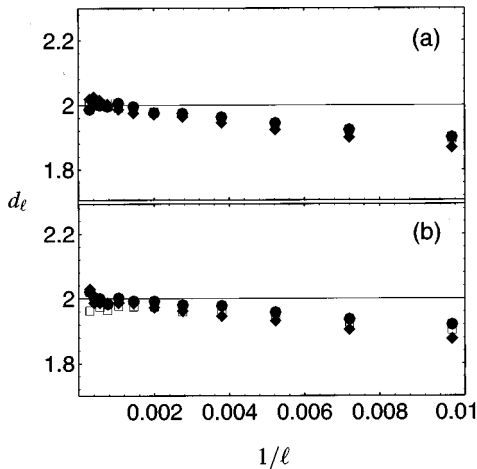


FIG. 12. Plot of the chemical dimension d_l as a function of $1/l$ [obtained from the successive slopes of $\log M(l)$ vs $\log l$] for (a) $z=3$, $(b,q)=(1,0.5)$ (full circle), $(b,q)=(0.5,0.4142)$ (square), and $(b,q)=(0.25,0.3333)$ (full diamond) and (b) $z=4$, $(b,q)=(1,0.6527)$ (full circle), $(b,q)=(0.5,0.5774)$ (square), and $(b,q)=(0.25,0.5)$ (full diamond). The horizontal lines represent the known value $d_l=2$ for percolation on a Cayley tree. The simulations were performed on a Cayley tree and averages were taken over 5×10^6 configurations.

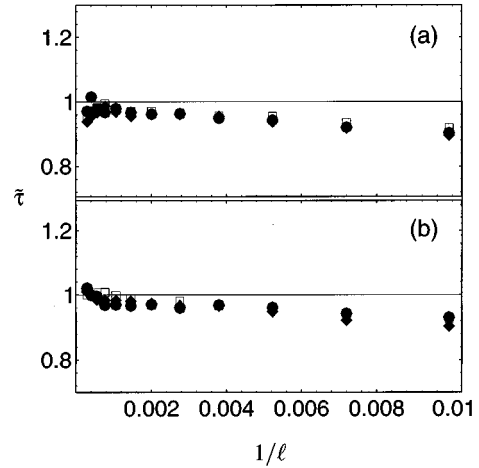


FIG. 13. Plot of the exponent $\tilde{\tau}$ as a function of $1/l$ [obtained from the successive slopes of $\log N(l)$ vs $\log l$] for the parameters described in Fig. 12. The horizontal lines represent the known value $\tilde{\tau}=1$ for percolation on a Cayley tree.

At the critical line, the second term in (10) vanishes [see Eq. (6)] and $p^*=1/(z-1)$, as in percolation on the Cayley tree. Hence $g(l)$ for the BPGM is, apart from a constant prefactor, the same as for percolation and thus all the critical exponents [which can be obtained from $g(l)$; see [14]] are the same as for percolation.

To test the convergence towards the analytical results we have performed extensive Monte Carlo simulations of the BPGM on the Cayley tree. Figures 12 and 13 show the chemical dimension d_l and the exponent $\tilde{\tau}$ of branched polymers on the Cayley tree as a function of the chemical distance l for (a) $z=3$ and (b) $z=4$, in both cases for three points on the critical line. We observe the expected behavior for large l , $M(l) \sim l^2$ and $N(l) \sim l^{-1}$.

V. DISCUSSION

From the three-dimensional simulations one cannot determine whether b_c for $q=0$ is finite or zero. However, we can present a heuristic argument that b_c is finite for any finite dimension d . Consider the case $q=0$, $b>0$, where KGWs are generated. For any finite dimension d there is a finite probability that the KGW will be trapped in a local cage and therefore the walk will finally terminate. This implies that the number of surviving walks of l steps, $N(l)$, decays exponentially as $N(l)/N(0) \sim \exp(-l/\xi_l)$, where $\xi_l \rightarrow \infty$ for $d \rightarrow \infty$.

Next we consider the case $q=0$, $b>0$. The characteristic length ξ_b between successive branchings is about $1/b$. For $\xi_l \ll \xi_b$, the growth will stop before branching occurs, while for $\xi_l \gg \xi_b$ we expect compact structures. From this we are led to assume that b_c is of the order of $1/\xi_l$. Indeed, our numerical estimate for ξ_l in $d=2$ is $\xi_l \approx 50$, which is of the order of magnitude of $1/b_c$. In $d=3$, ξ_l is about 10^4 . This indicates that b_c is of the order of 10^{-4} , which is beyond the detection of the available computers. On the Cayley tree, we have $\xi_l = \infty$ and thus $b_c = 0$, in agreement with our analytical calculations.

Finally, we like to mention that a quite similar model has been proposed by [15], but because of the small systems studied the exponents could not be identified. In addition, a

somewhat similar phase diagram was obtained from an Eden-type growth model, where the sites are blocked with probability q and the growth sites are active forever with a probability b or active for finite time τ_0 with probability $1-b$ [16]. Similar to the BPGM, there exists a critical line that separates SAW structures from compact structures and on the critical line the structures belong to the universality class of percolation.

ACKNOWLEDGMENTS

We like to thank Dr. S. Rabinovich, Dr. H.E. Roman, and A. Ordemann for valuable discussions. This work has been supported by the Minerva Center for the Physics of Mesoscopes, Fractals and Neural Networks; the Alexander-von-Humboldt Foundation; and the Deutsche Forschungsgemeinschaft.

-
- [1] P.J. Flory, *Principles of Polymer Chemistry* (Cornell University Press, Ithaca, 1953).
- [2] P.-G. de Gennes, *Scaling Concepts in Polymer Physics* (Cornell University Press, Ithaca, 1979).
- [3] P. Munk, *Introduction to Macromolecular Science* (Wiley, New York, 1989).
- [4] M. Doi and S.F. Edwards, *The Theory of Polymer Dynamics* (Oxford University Press, Oxford, 1986).
- [5] H.J. Herrmann, *Phys. Rep.* **136**, 153 (1986).
- [6] M. Daoud, in *Fractals in Science*, edited by A. Bunde and S. Havlin (Springer, Berlin, 1994).
- [7] T.C. Lubensky and J. Isaacson, *Phys. Rev. Lett.* **41**, 829 (1978).
- [8] S. Havlin, Z.V. Djordjevic, I. Majid, and H.E. Stanley, *Phys. Rev. Lett.* **53**, 178 (1984).
- [9] I. Majid, N. Jan, A. Coniglio, and H.E. Stanley, *Phys. Rev. Lett.* **52**, 1257 (1984).
- [10] J.W. Lyklema, in *Fractals in Physics*, edited by L. Pietronero and E. Tosati (North-Holland, Amsterdam, 1984); K. Kremer and J.W. Lyklema, *Phys. Rev. Lett.* **55**, 2091 (1985).
- [11] S. Havlin, B. Trus, and H.E. Stanley, *Phys. Rev. Lett.* **53**, 1288 (1984).
- [12] L.S. Lucena, J.M. Araújo, D.M. Tavares, L.R. da Silva, and C. Tsallis, *Phys. Rev. Lett.* **72**, 230 (1994).
- [13] A. Bunde, S. Havlin, and M. Porto, *Phys. Rev. Lett.* **74**, 2714 (1995).
- [14] *Fractals and Disordered Systems*, edited by A. Bunde and S. Havlin (Springer, Berlin, 1996).
- [15] S. Redner, *J. Phys. A* **12**, L239 (1979).
- [16] S. Miyazima, A. Bunde, S. Havlin, and H.E. Stanley, *J. Phys. A* **19**, L1159 (1986); A. Bunde, S. Miyazima, and H.E. Stanley, *J. Stat. Phys.* **47**, 1 (1987).